



HAL
open science

Functional characterization of GNAS mutations found in patients with pseudohypoparathyroidism type Ic defines a new subgroup of pseudohypoparathyroidism affecting selectively Gs α -receptor interaction

Susanne Thiele, Luisa de Sanctis, Ralf Werner, Joachim Grötzinger, Cumhur Aydin, Harald Jüppner, Murat Bastepe, Olaf Hiort

► To cite this version:

Susanne Thiele, Luisa de Sanctis, Ralf Werner, Joachim Grötzinger, Cumhur Aydin, et al.. Functional characterization of GNAS mutations found in patients with pseudohypoparathyroidism type Ic defines a new subgroup of pseudohypoparathyroidism affecting selectively Gs α -receptor interaction. Human Mutation, 2011, 10.1002/humu.21489 . hal-00631260

HAL Id: hal-00631260

<https://hal.science/hal-00631260>

Submitted on 12 Oct 2011

HAL is a multi-disciplinary open access archive for the deposit and dissemination of scientific research documents, whether they are published or not. The documents may come from teaching and research institutions in France or abroad, or from public or private research centers.

L'archive ouverte pluridisciplinaire **HAL**, est destinée au dépôt et à la diffusion de documents scientifiques de niveau recherche, publiés ou non, émanant des établissements d'enseignement et de recherche français ou étrangers, des laboratoires publics ou privés.



Functional characterization of GNAS mutations found in patients with pseudohypoparathyroidism type Ic defines a new subgroup of pseudohypoparathyroidism affecting selectively Gsa-receptor interaction

Journal:	<i>Human Mutation</i>
Manuscript ID:	humu-2010-0593.R1
Wiley - Manuscript type:	Research Article
Date Submitted by the Author:	27-Jan-2011
Complete List of Authors:	Thiele, Susanne; University of Lubeck, Department of Pediatrics De Sanctis, Luisa; University of Turin, Department of Pediatrics Werner, Ralf; University of Lubeck, Department of Pediatrics Grötzinger, Joachim; Christian Albrechts University of Kiel, Institute of Biochemistry Aydin, Cumhur; Gülhane School of Medicine, Center Dental Sciences Jüppner, Harald; General Hospital and Harvard Medical School, Departments of Medicine and Pediatrics Bastepe, Murat; General Hospital and Harvard Medical School, Departments of Medicine and Pediatrics Hiort, Olaf; University of Lubeck, Department of Pediatrics
Key Words:	Pseudohypoparathyroidism type Ia, Pseudohypoparathyroidism type Ic, Albright hereditary Osteodystrophy, Gsa protein activity

SCHOLARONE™
Manuscripts

1
2 1 **Functional characterization of *GNAS* mutations found in patients with**
3
4 2 **pseudohypoparathyroidism type Ic defines a new subgroup of**
5
6 3 **pseudohypoparathyroidism affecting selectively *Gsα*-receptor interaction**
7
8 4

9
10 5 Abbreviation title: Functional analysis of *GNAS* mutations in PHP1c

11 6 Thiele S¹, de Sanctis L², Werner R¹, Grötzinger J⁴, Aydin C^{3,5}, Jüppner H³, Bastepe M³, Hiort

12 7 O¹

13 8 ¹) Department of Pediatrics and Adolescent Medicine, University of Lübeck, Germany,

14 9 ²) Department of Pediatrics, University of Turin, Italy,

15 10 ³) Endocrine Unit, Massachusetts General Hospital and Harvard Medical School, Boston,

16 11 USA,

17 12 ⁴) Institute of Biochemistry, Christian-Albrechts-University of Kiel, Germany,

18 13 ⁵) Department of Endodontics, Center for Dental Sciences, Gülhane School of Medicine,

19 14 Ankara, Turkey

20 15
21
22 16 **Address all correspondence and requests for reprints to:**

23 17 Susanne Thiele, MD

24 18 Division of Pediatric Endocrinology and Diabetes,

25 19 Department of Pediatrics and Adolescent Medicine

26 20 University of Lübeck

27 21 Ratzeburger Allee 160

28 22 23538 Lübeck, Germany

29 23 Fon: +49-451-500-2191

30 24 Fax: +49-451-500-6867

31 25 e-mail: thiele@paedia.ukl.mu-luebeck.de

26 DISCLOSURE STATEMENT: The authors have nothing to disclose.

27 Abbreviations: Pseudohypoparathyroidism (PHP), Pseudohypoparathyroidism type Ia

28 (PHPIa), α -subunit of the stimulatory G protein ($G\alpha$), Pseudohypoparathyroidism type Ic

29 (PHPIc), Albright hereditary osteodystrophy (AHO), mouse $G\alpha$ -null fibroblast-like cell line

30 ($Gnas^{E2-/E2-}$), G protein-coupled receptor (GPCR), Pseudopseudohypoparathyroidism

31 (PPHP), Pseudohypoparathyroidism type Ib (PHPIb), guanosine 5'-[γ -thio]triphosphate

32 ($GTP\gamma_s$), human TSH receptor (TSHR), human PTH receptor (PTHr), Cholera toxin (CTX),

33 Isoproterenol (Iso), human [Y^{34}]PTH(1-34)amide (hPTH),

34 Word count: Text: 4273; Abstract: 198; Figures: 3; Tables: 3

Deleted: 69

Deleted: 4081

For Peer Review

51 **Abstract**

52 **Objective:** Pseudohypoparathyroidism type Ia (PHPIa) is caused by *GNAS* mutations
53 leading to deficiency of the α -subunit of stimulatory G proteins ($G\alpha$) that mediate signal
54 transduction of G protein-coupled receptors via cAMP. PHP type Ic (PHPIc) and PHPIa
55 share clinical features of Albright hereditary osteodystrophy (AHO); however, *in-vitro*
56 activity of solubilized $G\alpha$ protein is normal in PHPIc but reduced in PHPIa. **Methods:** We
57 screened 32 patients classified as PHPIc for *GNAS* mutations and identified three mutations
58 (p.E392K, p.E392X, p.L388R) in four unrelated families. These and one novel mutation
59 associated with PHPIa (p.L388P) were introduced into a pcDNA3.1(-) expression vector
60 encoding $G\alpha$ wild-type and expressed in a $G\alpha$ -null cell line ($Gnas^{E2-/E2}$). To investigate
61 receptor-mediated cAMP accumulation, we stimulated the endogenous expressed β_2 -
62 adrenergic receptor, or the co-expressed PTH- or TSH receptors, and measured the
63 synthesized cAMP by RIA. The results were compared to receptor-independent cholera
64 toxin-induced cAMP accumulation. **Results:** Each of the mutants associated with PHPIc
65 significantly reduced or completely disrupted receptor-mediated activation, but displayed
66 normal receptor-independent activation. In contrast, PHPIa associated p.L388P disrupted
67 both receptor-mediated activation and receptor-independent activation. **Conclusions:** We
68 present a new subgroup of PHP that is caused by $G\alpha$ deficiency and selectively affects
69 receptor-coupling functions of $G\alpha$.

70 **Key Words:** Pseudohypoparathyroidism type Ia, Pseudohypoparathyroidism type Ic,
71 Albright hereditary osteodystrophy, $G\alpha$ protein activity, $Gnas^{E2-/E2}$

76 **Introduction**

77 The term pseudohypoparathyroidism (PHP) describes a group of related rare disorders
78 characterized by end organ-resistance to PTH and other peptide hormones that mediate their
79 actions through G protein-coupled receptors (GPCRs) via cAMP/ protein kinase A. Based on
80 clinical and laboratory findings, and on the result of G α protein activity *in-vitro*, PHP has
81 been divided into different subgroups. PHP type Ia (PHPIa, MIM: 103580) is commonly
82 caused by heterozygous, maternally inherited inactivating mutations involving those exons of
83 the *GNAS* locus (MIM: 610540) that encode the α -subunit of the stimulatory G protein (G α).

84 These mutations lead to G α deficiency. Because there are some imprinted tissues where this
85 signaling protein is derived only or predominantly from the maternal allele, including
86 proximal renal tubules, thyroid, ovaries, and pituitary, affected individuals develop PTH-
87 resistance leading to hypocalcemia and hyperphosphatemia, as well as resistance towards
88 TSH and, sometimes, other peptide hormones and ligands. Due to haploinsufficiency of G α
89 in non-imprinted tissues, patients affected by PHPIa develop additional features of Albright
90 hereditary osteodystrophy (AHO), which include round face, short stature, brachymetacarpia,
91 ectopic ossification, and mental retardation. Patients also sometimes present with obesity.

92 Paternally inherited *GNAS* mutations lead to pseudo-PHP (PPHP, MIM: 612463)
93 characterized by some features of AHO in the absence of hormone resistance (reviewed in
94 Weinstein et al., 2002; Bastepe and Jüppner, 2005; Bastepe, 2008). Both, PHPIa and PPHP,
95 show diminished G α protein activity as determined by an *in vitro* assay using solubilized
96 G α from readily accessible cells such as red blood cells or fibroblasts and non-hydrolyzable
97 guanosine 5'-[γ -thio]triphosphate (GTP γ s) (Levine et al., 1980, 1988). G α protein activity
98 measurement has often been described as the first diagnostic step, followed by a molecular
99 genetic analysis of *GNAS*.

Deleted: in

Deleted: . A

Deleted: P

Deleted: usually

Deleted: in

1
2 100 PHP type Ib (PHPIb, MIM: 603233) is associated with the loss of methylation at one or more
3
4 101 maternally methylated regions within *GNAS* and can be caused by heterozygous, maternally
5
6 102 inherited deletions up-stream of or within the *GNAS* locus or can occur sporadically (Jüppner
7
8 103 et al., 1998, 2006; Bastepe et al., 2001). As a result, *Gsα* expression is reduced in a few
9
10 104 tissues including the renal proximal tubules and, in some cases, the thyroid, leading to PTH-
11
12 105 resistant hypocalcemia and hyperphosphatemia and occasionally elevated TSH levels.

13
14 106 Typically, PHPIb patients lack AHO features and present with normal *Gsα* activity (Bastepe,
15
16 107 2008). Recently, patients with PHP and AHO features have been described in association
17
18 108 with methylation changes of *GNAS* (de Nanclares et al., 2007; Mantovani et al., 2010), which
19
20 109 are not included in the current classification of the disorders.

Formatted: English (U.S.)

Formatted: English (U.S.)

Deleted: ed

Formatted: English (U.S.)

Deleted: has been described

Deleted: can not be

21
22 110 Pseudohypoparathyroidism type Ic (PHPIc, MIM: 612462) describes individuals who
23
24 111 develop the same clinical and laboratory abnormalities as patients with PHPIa, including
25
26 112 AHO and peptide hormone resistance, but in contrast to PHPIa, *in-vitro* assessment of *Gsα*
27
28 113 protein activity reveals no abnormality (table 1) (Weinstein, 1998). It has therefore been
29
30 114 postulated that PHPIc may not be caused by a functional impairment of the *Gsα* protein, but
31
32 115 by another component of the cAMP-dependent signaling pathway, such as adenylyl cyclase,
33
34 116 inhibitory G proteins, or phosphodiesterases (Farfel et al., 1981; Lania et al., 2001; Aldred,
35
36 117 2006; Mantovani and Spada, 2006).
37
38 118 We screened a cohort of patients classified as PHPIc (based on clinical and laboratory data
39
40 119 and the result of the *in-vitro* assay) and found mutations in the *GNAS* gene in a subgroup. We
41
42 120 then performed functional analysis of three naturally occurring mutations located in the
43
44 121 extreme C-terminus of *Gsα*. By analyzing the receptor-mediated activation of the *Gsα*-
45
46 122 mutants in a mouse *Gsα*-null fibroblast-like cell line (*Gnas*^{E2-/E2-}) and comparing the results
47
48 123 to receptor-independent activation, we demonstrate that these mutations selectively affect
49
50
51
52
53
54
55
56
57
58
59
60

1
2 124 receptor-coupling but not adenylyl cyclase activating functions of $G\alpha$, while the *PHPIa*
3
4 125 associated mutation affects both.
5
6 126
7

8 127 **Patients and methods**
9

10 128 We screened 32 patients with PHP, AHO and normal measured $G\alpha$ protein activity for
11 129 mutations in exons 1-13 of *GNAS* including exon/intron boundaries. Here, we only describe
12 130 the phenotype and history of patients in whom we found *GNAS* mutations. The clinical and
13 131 laboratory data are summarized in table 2
14
15
16
17

18 132 **Patient A:** The male patient was delivered at term after an uneventful pregnancy by
19 133 Caesarian section. During birth he suffered from asphyxia, which was initially thought to be
20 134 the cause of a delay of his speech and psychomotoric development. At the age of 12 years, he
21 135 was hospitalized because of facial nerve palsy. He showed characteristic AHO features,
22 136 including round face, shortening of the 4th and 5th metacarpals and mental retardation with an
23 137 IQ of 40 (assessed by HAWIK). His mother had only mild signs of AHO, including short
24 138 stature (154 cm, <3rd centile), and brachymetacarpia of the 4th metacarpals, but no other
25 139 AHO features, and no evidence for hormonal resistance, consistent with the diagnosis of
26 140 PPHP. The patient does not have siblings and the father is healthy.
27
28
29
30
31
32
33
34
35

36 141 **Patient B:** The female patient was born at term after an uneventful pregnancy as the only
37 142 child of their parents. AHO and PHP were diagnosed at the age of 5.5 years when she
38 143 presented at the endocrine clinic with round face, brachymetacarpia of the 3rd, 4th, and 5th
39 144 metacarpals and obesity (22.5 kg, BMI 19.6 kg/ m², >97th centile). Her mother presented with
40 145 brachymetacarpia but no other AHO features and PTH and TSH levels were in the normal
41 146 range, consistent with the diagnosis of PPHP. The father did not present any AHO signs.
42
43
44
45
46
47

48 147 **Patient C:** The patient is a female, born at 38 weeks of gestation as the only child of their
49 148 parents. Diagnosis of AHO and PHP was suspected because of neonatal hypothyroidism. At
50
51
52
53
54
55
56
57
58
59
60

1
2 149 11 months of age she had a round face, her length was 65.5 cm (<3rd centile), she had already
3
4 150 developed brachymetacarpia affecting the 4th and 5th phalanges and her weight was 7.8 kg
5
6 151 (BMI 18,4 kg/m², 90th centile). Her mother was of short stature (142 cm, <3rd centile) and had
7
8 152 also brachymetacarpia, but no hormonal resistances.

10 153 **Patient D1:** The patient is a male twin born at term. He came for endocrinological
11
12 154 assessment at the age of 13 years because of recurrent hypocalcemia, and presented with
13
14 155 round face and brachymetacarpia of the 4th and 5th phalanges.

Deleted: ,

Deleted: ,

Deleted: born at term,

16 156 **Patient D2:** The patient is the twin sister of D1, with an uneventful medical history until the
17
18 157 age of 13 years. At this time, her weight was slightly elevated (55 kg, BMI 26.5 kg/m², 97th
19
20 158 centile) and she presented with round face and brachymetacarpia. The mother of both
21
22 159 children had a round face, was of short stature (152 cm, <3rd percentile), and demonstrated
23
24 160 brachymetacarpia of the 4th and 5th metacarpals and metatarsals, but no hormonal alterations
25
26 161 or further AHO signs. The father of both children is healthy.

28 162 **Patient E:** The female patient was born after uneventful pregnancy. She was hospitalized at
29
30 163 the age of 4 years when she presented with hypocalcemic seizures. At this time she
31
32 164 demonstrated a round face, brachymetacarpia of the 5th metacarpals, and obesity (20.7 kg,
33
34 165 >97th centile), but no other signs of AHO. Her mother also presented with short 5th
35
36 166 metacarpals, however, PTH and TSH levels were in the normal range. The patient does not
37
38 167 have siblings and the father does not show abnormalities.

40 168 Patients B, D1 and D2 have in part already been described by de Sanctis (de Sanctis et al.,
41
42 169 2003).

44 170 Laboratory investigations at the time of diagnosis revealed for all patients elevated PTH and
45
46 171 TSH levels. Vitamin D deficiency had been excluded before by measuring 25-OH-vitamin D
47
48 172 levels within the reference range. The *in-vitro* Gsa activity was normal, except for patient E,
49
50 173 (activity was reduced to 71%), when compared to healthy controls. All subjects or their

174 guardians gave informed consent to the study. Studies were approved by the ethical
175 committee of the University of Lübeck as part of the funded project on AHO (see
176 acknowledgment).

177

178 G α protein activity and mutation analysis

179 The activity of G α protein from erythrocyte membranes of patients was investigated in
180 heparinized blood samples as described earlier (Levine et al., 1980; Ahrens et al., 2001).
181 Briefly, after solubilization the G α protein from patient derived erythrocyte membranes was
182 incubated with GTP γ S. We added adenylyl cyclase from turkey red cell membranes and
183 measured the generated cAMP in the presence of ATP by RIA (Immuno Biological
184 Laboratories, Hamburg, Germany). Results obtained in triplicate were expressed as percent of
185 the mean of healthy controls (normal range: 85–115 %). For molecular genetic analysis we
186 isolated genomic DNA derived from peripheral leukocytes by standard procedures (Qiaquick
187 DNA kit, Qiagen, Hilden, Germany). *GNAS* exon 1-13, (RefSeq NM_000516.4) including all
188 intron/exon boundaries were amplified in 11 fragments by PCR (primer sequences available
189 upon request). PCR-amplified DNA was sequenced by direct cycle sequencing using the
190 BigDye Terminator v1.1 Cycle Sequencing Kit (Applied Biosystems, Foster City, CA) and
191 an ABI 3130 capillary sequencer (Applied Biosystems, Foster City, CA).

192

193 Site-directed mutagenesis of expression plasmids

194 We introduced the detected mutations p.E392K, p.E392X, p.L388R and p.L388P into a
195 pcDNA3.1(-) vector encoding wild-type rat G α (which is identical to human G α), in which
196 a shortened hemagglutinine epitope-tag (DVPDYA) had been introduced into exon 3 by
197 PCR-based mutagenesis (Bastepe et al., 2002). The first PCR amplification was carried out
198 by using a sense primer in exon 4 and an antisense primer comprising the respective

1
2 199 mutation. A second PCR was performed using a sense primer containing the mutation and an
3
4 200 antisense primer (Bgh-as) located downstream of G α . PCR products were used as a template
5
6 201 in a third PCR using the exon 4-sense and the Bgh-antisense primer. PCR products were
7
8 202 amplified in a Mastercycler Gradient (Eppendorf, Hamburg, Germany) using the following
9
10 203 cycling protocol: denaturation for 30 s at 98 C, followed by 29 cycles denaturation (10 s at 98
11
12 204 C), annealing (30 s at 64 C), and elongation (45 s at 72 C) and 1 final cycle (10 min at 72 C).
13
14 205 The reaction mix contained 100 ng vector DNA, 1x Phusion-buffer HF, 2.5 U Phusion High-
15
16 206 Fidelity DNA-Polymerase (New England Biolabs) and 200 μ M dNTPs (Fermentas, St. Leon-
17
18 207 Rot, Germany). The amplicon including the respective mutation was double digested with
19
20 208 *AfeI* and *HindIII* (New England Biolabs, Beverley, CA) and subcloned into the original G α
21
22 209 expression vector. All clones were verified by nucleotide sequence analysis including the
23
24 210 entire inserts up to cloning borders.

25
26 211 .
27
28 212 Cell culture, transfection, and stimulation
29
30 213 For transfection experiments, we used Gnas^{E2-/E2-} cells, a clonal murine cell line in which
31
32 214 *Gnas* exon 2 had been disrupted and thus does not express endogenous G α or XLAs (Bastepe
33
34 215 et al., 2002). Cells were seeded into 24-well plates at a density of 60-80 %. After 24 h, the
35
36 216 cells were transfected with 0.2 μ g/well of plasmid DNA encoding G α using Effectene
37
38 217 (Qiagen, Valencia, CA). For cotransfection experiments with plasmids encoding the human
39
40 218 TSH receptor (TSHR) or the human PTH receptor (PTHr), the total amount of DNA per well
41
42 219 was 0.4 μ g, which was kept constant by addition of empty vector. Cells were cultured at 37 C
43
44 220 for 72 h with daily exchanges of DMEM-F12-medium containing 10 % fetal bovine serum
45
46 221 followed by stimulation with different agonists. For determination of cholera toxin (CTX)-
47
48 222 induced cAMP formation, cells were treated at 37 C for 2 h with 1 μ g/ml CTX (Sigma-
49
50 223 Aldrich Corp., St. Louis, MO). Stimulation with Isoproterenol (Sigma-Aldrich Corp., St.

1
2 224 Louis, MO), human [Y^{34}]PTH(1-34)amide (PTH) (Massachusetts General Hospital,
3
4 225 Biopolymer Core Facility, Boston, USA) and human TSH (Sigma-Aldrich Corp., St. Louis,
5
6 226 MO) were carried out in the presence of F12-DMEM containing HEPES-NaOH, 1 mg/ml
7
8 227 BSA, and 2 mM isobutylmethylxanthine (Sigma-Aldrich Corp., St. Louis, MO). Treatment
9
10 228 was followed by 15 min incubation at 37 C in a water bath. After incubation cells were lysed
11
12 229 by 50 nM HCl and cAMP accumulation in each well was determined by RIA as previously
13
14 230 described (Bastepe et al., 2002). All transfection experiments in this study were repeated at
15
16 231 least three times.

17 232

20 233 Western blot analysis

22 234 For Western blot analysis, 15 μ g of cellular protein were loaded onto a 12 % polyacrylamide
23
24 235 gel. Electrophoresis was carried out at 100 V for 120 min in a Mini-Protean 3 chamber
25
26 236 (BioRad, Munich, Germany). Proteins were transferred to nitrocellulose membranes (BA85,
27
28 237 Schleicher & Schüll, Dassel, Germany) at 100 V for 80 min using a Mini Trans-Blot cell
29
30 238 (BioRad, Munich, Germany) and using a blotting buffer containing 16.5 mM Tris, 150 mM
31
32 239 glycine and 20 % (V/V) methanol. Non-specific binding sites were blocked by immersing the
33
34 240 membranes overnight at 4 C in 5% non-fat milk (Becton-Dickinson, Franklin Lakes, USA)
35
36 241 dissolved in PBS/ Tween buffer (containing 137 mM NaCl, 2.7 mM KCl, 10 mM Na₂HPO₄,
37
38 242 2 mM KH₂PO₄, 0.1 % Tween 20, pH 7.4). The blocked membranes were incubated with an
39
40 243 HA-antibody (Y11: sc805, Santa Cruz Biotechnology) diluted 1:100 in blocking buffer for 1
41
42 244 h at room temperature. The membrane was rinsed 4 times for 15 min in PBS/Tween buffer
43
44 245 and incubated with an anti-rabbit IgG peroxidase conjugate at a dilution of 1:1000 (Sigma,
45
46 246 Taufkirchen, Germany) for 1 h. After rinsing the membrane as above, protein bands were
47
48 247 visualized using the Western Lightning Chemiluminescence Reagent Plus substrate (Perkin
49
50
51
52
53
54
55
56
57
58
59
60

1
2 248 Elmer, Boston, MA) and the Fusion SL detection system (Vilber Lourmat, Eberhardzell,
3
4 249 Germany).

5
6 250

7
8 251 Statistical analysis and structural analysis

9
10 252 Student's *t* test for two independent samples was used to determine significance of observed
11
12 253 differences of the cAMP levels after CTX-mediated stimulation of Gs α -388R (corresponding
13
14 254 to the p.L388R mutant of Gs α) and Gs α -388P and after Isoproterenol-mediated stimulation of
15
16 255 Gs α -392K and Gs α -392X. GraphPad 4.0 was used for determination of the EC₅₀. For the
17
18 256 structural analysis the crystal structure of Gs α in complex with GTP γ -s (Sunahara et al.,
19
20 257 1997) has been used. The structural representations were generated using the RIBBONS
21
22 258 software (Kraulis, 1991).

23
24 259

25
26 260 **Results**

27
28 261 In 5 patients with PPH1c from 4 unrelated families our analysis of *GNAS* (RefSeq
29
30 262 NM_000516.4) revealed 3 different heterozygous mutations in exon 13 affecting the two
31
32 263 residues 388 and 392 in the carboxy-terminal portion of Gs α . In addition, we found one
33
34 264 further mutation also affecting the residue 388, but associated with PPH1a.
35
36 265 In patient A and his mother, a single nucleotide exchange in codon 388 (c.1163T>G) was
37
38 266 identified, leading to an arginine instead of a leucine (p.L388R). This mutation has not been
39
40 267 described so far. A missense mutation in codon 392 (c.1174G>A) was identified in patient C
41
42 268 and her mother, resulting in a substitution of glutamic acid by lysine (p.E392K). In patient B,
43
44 269 D1, and D2 and their mothers we confirmed the heterozygous nucleotide change
45
46 270 (c.1174G>T) at codon 392 in concordance to the previously results in these patients (de
47
48 271 Sanctis et al., 2003) resulting in a stop codon (p.E392X). In patient E and her mother
49
50 272 (PPH1a), we also found a novel heterozygous change at codon 388 (c.1163T>C) resulting in

273 proline instead of a leucine (p.L388P). [Nucleotide numbering reflects cDNA numbering](#)
 274 [system with +1 corresponding to the A of the ATG translation initiation codon in the](#)
 275 [reference sequence \(NM_000516.4\), according to the journal guidelines](#)
 276 [\(www.hgvs.org/mutnomen\)](http://www.hgvs.org/mutnomen).

277 The analysis of the remaining 27 patients with PHP1c did not reveal mutations in the G α
 278 encoding region of *GNAS*. All variants were not detected in 100 normal individuals and all
 279 involve highly conserved amino acids (table 3). The mutations are summarized in table 2.

280 The mutations were included in the [Leiden Open Variation Database](#)
 281 [\(http://www.lovd.nl/GNAS\)](http://www.lovd.nl/GNAS), according to the nomenclature of the HGVS site. In this report,
 282 however, the commonly used nomenclature of Kosaza et al. (1988) has been used.

Deleted: LOVD

Deleted: data base

284 First we studied the ability of the missense mutants G α -388R and G α -392K (corresponding
 285 to p.L388R and p.E392K encoded in the G α -encoding vector) to be stimulated by the β_2 -
 286 adrenergic receptor expressed endogenously in our Gnas^{E2-/E2-} fibroblast-like cells. Receptor
 287 mediated cAMP accumulation in response to 10⁻⁵M Isoproterenol was measured after
 288 transient expression of mutant or wild-type G α . The results were compared to CTX-induced
 289 cAMP accumulation, which stimulates adenylyl cyclase by ADP-ribosylation independent of
 290 receptor activation (CTX-stimulated wild-type G α was set as maximal stimulation of 100%).
 291 After Isoproterenol stimulation G α -388R failed to induce any increase in intracellular cAMP
 292 (mean 4.5 %, SEM \pm 0.3), compared to the basal cAMP level (mean 3.6 % of max, SEM
 293 \pm 1.1), despite nearly normal CTX-induced cAMP levels (mean 81.1 % of max, SEM \pm 8.2).
 294 In contrast, G α -392K was activated by Isoproterenol, but maximal cAMP levels were only
 295 about 50% of wild-type (mean 43.6% of max, SEM \pm 3), whereas the CTX-induced cAMP
 296 accumulation was comparable to that of the wild-type (mean 105.6 %, SEM \pm 8.3) (figure 1a).
 297 Non-transfected cells or cells transfected with the empty pcDNA3.1(-) vector, which were

1
2 298 used as negative controls, failed to show an increase in basal, CTX- and Isoproterenol-
3
4 299 stimulated cAMP levels (data not shown).
5
6 300 To determine whether cAMP accumulation of the wild-type and the mutants is dependent on
7
8 301 agonist levels, we stimulated the cells with concentrations of Isoproterenol ranging from 10^{-4}
9
10 302 to 10^{-8} M. Isoproterenol treatment increased cAMP formation in a dose-dependent manner in
11
12 303 cells transiently expressing the wild-type Gs α ($EC_{50}=10^{-5.895}$ M; 95 % confidence interval $10^{-5.979}$
13
14 304 to $10^{-5.811}$). Consistent with our previous experiments, Isoproterenol failed completely to
15
16 305 increase cAMP generation in cells transiently expressing Gs α -388R (mean 5.8 %, SEM
17
18 306 ± 0.2). Gs α -392K led to a significant increase in cAMP formation in response to agonist
19
20 307 treatment with EC_{50} values ($EC_{50}=10^{-5.995}$ M; 95 % confidence interval $10^{-6.108}$ to $10^{-5.883}$)
21
22 308 similar to wild type Gs α ; however, maximal response after stimulation with 10^{-4} M was
23
24 309 reduced to about 50 % (mean 49.8 %, SEM ± 4.4) (figure 1b).

Deleted: similar

Deleted: as Gs α -388R ($EC_{50}=10^{-5.995}$ M;
95 % confidence interval $10^{-6.108}$ to $10^{-5.883}$)

Deleted: was

25
26 310
27
28 311 Since all patients presented with PTH resistance, experiments with cells transiently
29
30 312 expressing both Gs α -mutants/wild-type and the PTHR were performed. Stimulation with 10^{-8}
31
32 313 M PTH revealed a similar pattern for Gs α -388R and Gs α -392K to that observed after
33
34 314 stimulation of the endogenous β_2 -receptor. Gs α -388R did not show any response after agonist
35
36 315 stimulation (mean 16.73 % of max, SEM ± 0.33) and Gs α -392K led to a diminished response
37
38 316 to about 60 % (mean 60.5 % of max, SEM ± 1.86) compared to the wild-type (mean 100 %, SEM
39
40 317 ± 3.31). These results were confirmed by dose dependent agonist stimulation (figure 1c).
41
42 318 The EC_{50} for PTH-induced cAMP accumulation through Gs α -392K ($10^{-9.307}$ M) was similar
43
44 319 as for wild-type Gs α ($10^{-9.102}$ M).
45
46 320 Furthermore, we cotransfected cDNA encoding the human TSHR and the vectors containing
47
48 321 the Gs α -mutants, and stimulated the cells with 10 mIU/ml TSH. Again, the Gs α -388R mutant
49
50 322 was unable to transduce receptor-mediated cAMP response, and Gs α -392K led to a

1
2 323 diminished response. Transfection with the empty vector, or the TSHR alone used as negative
3
4 324 controls did not elevate the cAMP levels after stimulation with TSH (results not shown).

5
6 325
7
8 326 To investigate whether our cell model can discriminate different functional effects of
9
10 327 mutations leading to the PHPIa or the PHPIc-subtype even if located in the same residue, we
11
12 328 transfected the $Gnas^{E2-/E2-}$ cells with $G\alpha$ -388P associated with PHPIa. We compared the
13
14 329 results to those of $G\alpha$ -388R. As $G\alpha$ -388R (mean 4.2 %, SEM \pm 1.2), $G\alpha$ -388P could not be
15
16 330 stimulated by Isoproterenol (mean 3.4 %, SEM \pm 1). However, in concordance to the reduced
17
18 331 $G\alpha$ protein activity in erythrocyte membranes leading to the diagnosis of PHPIa in this
19
20 332 patient, the CTX-induced stimulation by $G\alpha$ -388P was reduced to nearly 60 % (mean 55.98
21
22 333 % of max, SEM \pm 2.95), compared to the wild-type (mean 100 %, SEM \pm 3.9). In contrast, the
23
24 334 CTX-induced stimulation of $G\alpha$ -388R was similar to the wild type (mean 92.48 %, SEM \pm 7)
25
26 335 (figure 2a).

27
28 336 We also investigated the nonsense mutation $G\alpha$ -392X found in our patients B, D1 and D2
29
30 337 and compared the results to those of the missense mutant $G\alpha$ -392K affecting the same
31
32 338 residue. In contrast to our findings in $G\alpha$ -392K (32.19 % of max, SEM \pm 0.14), we could not
33
34 339 demonstrate any significant stimulation via the β_2 -receptor in $G\alpha$ -392X (mean 7.32 % of
35
36 340 max, SEM \pm 0.36) (figure 2b).

37
38 341
39
40 342 The CTX-induced cAMP accumulation of the PHPIc associated mutants $G\alpha$ -388R, $G\alpha$ -
41
42 343 392K, and $G\alpha$ -392X did not show significant differences to the wild-type, but the PHPIa
43
44 344 associated mutant $G\alpha$ -388P led to diminished CTX-induced cAMP synthesis. To rule out
45
46 345 different expression levels between $G\alpha$ -388P and the wild-type $G\alpha$, we established
47
48 346 immunoblot analysis using hemagglutinine-tag specific antibody and demonstrated

1
2 347 equivalent expression of all mutants except a slightly reduced expression of Gsa-392X
3
4 348 (figure 2c).

5
6 349

7
8 350 **Discussion**

9
10 351 Historically, the term PHPIc has been used for a constellation including PHP, AHO signs and
11
12 352 a normal Gsa activity measured *in-vitro*. Therefore, PHPIc is thought to be caused by
13
14 353 impairment of another component of the cAMP-dependent pathway than Gsa (Aldred, 2006;
15
16 354 Mantovani and Spada, 2006). In our study we demonstrate in a subset of patients with the
17
18 355 former diagnosis PHPIc inherited maternal inactivating mutations in the Gsa encoding exons
19
20 356 of *GNAS*. Furthermore, we prove impaired interaction between different GPCRs and the
21
22 357 mutated Gsa forms leading to deficient Gsa signalling. Since these mutations lead, in contrast
23
24 358 to classical PHPIc, to Gsa deficiency and affect, in contrast to PHPIa, selectively Gsa-
25
26 359 receptor coupling functions, this constitutes a new subgroup of PHP based on distinct
27
28 360 molecular dysfunction of Gsa.

29
30 361

31
32 362 Two further patients harboring *GNAS* mutations with similar functional deficits have been
33
34 363 described. The nonsense mutation p.Y391X was identified in a PHPIc patient (Linglart et al.,
35
36 364 2002) and molecular investigation of this Gsa-mutant led to the proposal that PHPIc
37
38 365 represents a subgroup of PHPIa in which the *GNAS* mutations affect receptor-coupling
39
40 366 (Linglart et al., 2006; Bastepe, 2008). The second described patient (harboring the mutation
41
42 367 p.R385H) also demonstrated impaired receptor-coupling without disturbing downstream Gsa
43
44 368 signaling. However, since the assay used for diagnosis did involve GPCR-Gsa coupling the
45
46 369 patient was termed as having PHPIa (Schwindinger et al, 1994).

47
48 370

1
2
3 371 All *GNAS* mutations found in our patients are located in the α 5-helix concerning the extreme
4
5 372 carboxyl-terminus of $G\alpha$ (which is highly conserved between different species, [see table 3](#)),
6
7 373 whereas usually PHPIa-associated mutations are distributed throughout the gene
8
9 374 (www.hgmd.cf.ac.uk). The results from a variety of studies implicate that this region contains
10
11 375 the major sites for interaction between $G\alpha$ and GPCRs (Sullivan et al., 1987; Masters et al.,
12
13 376 1988; Spiegel et al., 1990; Pantoloni et al., 1993; Rasenick et al., 1994; Hamm et al., 1998;
14
15 377 Linglart et al., 2006; Zang et al., 2006). Consistent with these results, our data demonstrate
16
17 378 that natural mutations located at the carboxy-terminal end of $G\alpha$ can disrupt or strongly
18
19 379 impair the ability for receptor-coupling despite normal CTX- or GTP γ S induced adenylyl
20
21 380 cyclase activity.

22 381
23
24 382 The $G\alpha$ -388R-mutant showed a complete loss of receptor-mediated stimulation of the β ₂-
25
26 383 adrenergic receptor, the PTHR, and the TSHR, indicating a crucial role of this residue for
27
28 384 receptor-coupling. We analyzed the three dimensional structure of *GNAS* that has been
29
30 385 described previously (Sunahara et al., 1997) to examine the putative effects of the mutation.
31
32 386 The hydrophobic side chain of L388 of the α 5-helix is part of the accessible surface of the
33
34 387 molecule and thus directly involved in contact of $G\alpha$ to the GPCR. The p.L388R will
35
36 388 introduce a positive charge at this position and thus interfere with receptor binding.
37
38 389 The mutation p.L388P, associated with PHPIa, also leads to a reduced response to receptor-
39
40 390 independent activation. Normally, the backbone amide group of L388 forms a hydrogen bond
41
42 391 with the carbonyl group of Q384. Since proline is, in contrast to arginine, not able to form
43
44 392 such a helix stabilizing hydrogen bond, the p.L388P mutation will lead to destabilization of
45
46 393 the α 5-helix and thereby may disturb the whole tertiary structure of the molecule and thus
47
48 394 reduce not only the receptor-dependent, but also the receptor-independent stimulation.

Deleted: (

1
2 395 The missense mutant Gs α -392K demonstrated a residual activity after receptor-coupled
3
4 396 stimulation with Isoproterenol, while in contrast the nonsense mutant Gs α -392X led to a
5
6 397 complete loss of receptor-mediated activation through β_2 -receptor stimulation. These results
7
8 398 seem to be reflected even by the severity of PTH and TSH resistance found in the patients
9
10 399 (see table 2). This strongly suggests that the last three amino acid residues of Gs α are
11
12 400 essential for receptor-coupling and the results are in agreement with the findings of Linglart,
13
14 401 who demonstrated a complete loss of the β_2 -adrenergic receptor-mediated activation by the
15
16 402 p.Y391X-mutant that lacks the last four residues of Gs α (Linglart et al., 2006). In addition,
17
18 403 the loss of the last three amino acids may lead to instability of the protein, as suggested by
19
20 404 slightly reduced expression of Gs α -392X in our Western blotting analysis (figure 2c).
21
22 405
23
24 406 Although, we identified *GNAS* mutations in a subset of designated PHPIc patients, the
25
26 407 ethiopathogenesis of the remaining 27 cases remains to be elucidated. In the literature, two
27
28 408 PHPIc patients have been described in whom the disease is caused by epigenetic changes
29
30 409 involving the *GNAS* locus (de Nanclares et al., 2007). However, several patients with the
31
32 410 diagnosis of PHPIc neither show epigenetic nor molecular genetic changes in *GNAS*,
33
34 411 demonstrating that PHPIc may be caused by a variety of pathogenetic mechanisms.
35
36 412
37
38 413 In summary, our molecular genetic and functional data prove impaired Gs α function by
39
40 414 naturally occurring mutations at the Gs α encoding exons of *GNAS* as one cause of patients
41
42 415 formerly diagnosed with PHPIc. However, since these mutations concern selectively Gs α -
43
44 416 receptor coupling functions and show fundamental differences from those mutations
45
46 417 associated with PHPIa, we regard this as a new subgroup of PHP. On the basis of our
47
48 418 findings and the findings of methylation changes in patients with PHP and AHO (de
49
50 419 Nanclares et al., 2007; Mantovani et al., 2010), a new classification of *GNAS* related

Deleted: In contrast to the

Deleted: t

Deleted: is

Deleted: s

Deleted: is even

Deleted: laboratory results

Deleted: affected

Deleted: ,

Deleted: in the future

Deleted: In the future

1
2 420 disorders should be proposed [in the future](#), based not only on clinical and laboratory
3
4 421 alterations, but also on molecular genetic, epigenetic, and functional changes.
5
6 422

7
8 423 **Acknowledgements**
9

10 424 We thank all family members for their participation, and their physicians for sending us the
11
12 425 samples. Moreover, we are grateful to Dagmar Struve, Christine Marschke, and Pia Staedt for
13
14 426 excellent technical assistance. This work was supported by research grants from the German
15
16 427 Ministry for Research and Education (BMBF No: GMG 01GM0315 to OH), a travel grant of
17
18 428 the Fritz Thyssen Stiftung (To ST) and a research grant to [LdS](#) (Piedmont Region Funds for
19
20 429 Finalized Research 2009, R4325). The study was furthermore supported by the Cluster of
21
22 430 Excellence “Inflammation at interfaces” (to JG). This work was also funded, in part, by
23
24 431 research grants from National Institute of Diabetes and Digestive and Kidney Diseases
25
26 432 (R01DK073911 to MB and R37DK46718 to HJ).
27
28 433
29
30 434
31
32 435
33
34
35
36
37
38
39
40
41
42
43
44
45
46
47
48
49
50
51
52
53
54
55
56
57
58
59
60

Deleted: L

436 **References:**

- 437 Ahrens W, Hiort O, Staedt P, Kirschner T, Marschke C, Kruse K. 2001. Analysis of the
438 *GNAS1* gene in Albright's hereditary osteodystrophy. *J Clin Endocrinol Metab*
439 86:4630-4634.
- 440 Aldred MA. 2006. Genetics of pseudohypoparathyroidism types Ia and Ic. *J Pediatr*
441 *Endocrinol Metab* 19(2):635-640.
- 442 Bastepe M, Pincus JE, Sugimoto T, Tojo K, Kanatani M, Azuma Y, Kruse K, Rosenbloom
443 AL, Koshiyama H, Jüppner H. 2001. Positional dissociation between the genetic
444 mutation responsible for pseudohypoparathyroidism type Ib and the associated
445 methylation defect at exon A/B: evidence for a long-range regulatory element within
446 the imprinted *GNAS1* locus. *Hum Mol Genet* 10:1231-1241.
- 447 Bastepe M, Gunes Y, Perez-Villamil B, Hunzelman J, Weinstein LS, Jüppner H. 2002.
448 Receptor-mediated adenylyl cyclase activation through XLalpha(s), the extra-large
449 variant of the stimulatory G protein alpha-subunit. *Mol Endocrinol* 16:1912-1919.
- 450 Bastepe M, Jüppner H. 2005. *GNAS* locus and pseudohypoparathyroidism. *Horm Res* 63:65-
451 74.
- 452 Bastepe M. 2008. The *GNAS* locus and pseudohypoparathyroidism. *Adv Exp Med Biol* 626:
453 27-40.
- 454 De Sanctis L, Romagnolo D, Olivero M, Buzi F, Maghnie M, Soire G, Crino A, Baroncelli
455 GI, Salerno M, Di Maio S, Cappa M, Grosso S, Rigon F, Lala R, De Sanctis C,
456 Dianzani I. 2003. Molecular analysis of the *GNAS1* gene for the correct diagnosis of
457 Albright hereditary osteodystrophy and pseudohypoparathyroidism. *Pediatr Res*
458 53:749-755.
- 459 de Nanclares GP, Fernández-Rebollo E, Santin I, García-Cuartero B, Gaztambide S,
460 Menéndez E, Morales MJ, Pombo M, Bilbao JR, Barros F, Zazo N, Ahrens W,

- 1
2 461 Jüppner H, Hiort O, Castaño L, Bastepe M. 2007. Epigenetic defects of GNAS in
3
4 462 patients with pseudohypoparathyroidism and mild features of Albright's hereditary
5
6 463 osteodystrophy. *J Clin Endocrinol Metab.* Jun;92(6):2370-2373.
7
8
9 464 Farfel Z, Brothers VM, Brickman AS, Conte F, Neer R, Bourne H. 1981.
10
11 465 Pseudohypoparathyroidism: Inheritance of deficient receptor-cyclase coupling
12
13 466 activity. *Proc Natl Acad Sci* 78: 3098-3102.
14
15 467 Hamm HE, Deretic A, Arendt A, Hargrave PA, Koenig B, Hofmann KP. 1998. Site of G
16
17 468 protein binding to rhodopsin mapped with synthetic peptides from the alpha subunit.
18
19 469 *Science* 241; 832-835.
20
21 470 Jüppner H, Schipani E, Bastepe M, Cole DE, Lawson ML, Mannstadt M, Hendy GN, Plotkin
22
23 471 H, Koshiyama H, Koh T, Crawford JD, Olsen BR, Vikkula M. 1998. The gene
24
25 472 responsible for pseudohypoparathyroidism type Ib is paternally imprinted and maps in
26
27 473 four unrelated kindreds to chromosome 20q13.3. *Proc Natl Acad Sci U S A* 95:11798-
28
29 474 11803.
30
31 475 Jüppner H, Linglart A, Fröhlich LF, Bastepe M. 2006. Autosomal-dominant
32
33 476 pseudohypoparathyroidism type Ib is caused by different microdeletions within or
34
35 477 upstream of the GNAS locus. *Ann N Y Acad Sci* 1068:250-255.
36
37 478 Kozasa T, Itoh H, Tsukamoto T, Kaziro Y 1988, Isolation and characterization of the human
38
39 479 Gs alpha gene. *Proc Natl Acad Sci U S A* 85: 2081-2085
40
41 480 Kraulis PJ. 1991. MOLSCRIPT: a program to produce both detailed and schematic plots of
42
43 481 protein structures. *Journal of Appl Crystallogr* 24:946-950.
44
45 482 Lania A, Mantovani G, Spada A. 2001. G protein mutations in endocrine diseases. *Eur J*
46
47 483 *Endocrinol* 145:543-559.
48
49 484 Levine MA, Downs RW Jr., Singer M, Marx SJ, Aurbach GD, Spiegel AM. 1980. Deficient
50
51 485 activity of guanine nucleotide regulatory protein in erythrocytes from patients with
52
53
54
55
56
57
58
59
60

- 1
2 486 pseudohypoparathyroidism. *Biochem Biophys Res Commun* 94:1319-1324.
- 3
4 487 Levine MA, Ahn TG, Klupt SF, Kaufman KD, Smallwood PM, Bourne HR, Sullivan KA,
5
6 488 Van Dop C. 1988. Genetic deficiency of the alpha subunit of the guanine nucleotide-
7
8 489 binding protein Gs as the molecular basis for Albright hereditary osteodystrophy. *Proc*
9
10 490 *Natl Acad Sci U S A* 85:617-621.
- 11
12 491 Linglart A, Carel JC, Garabedian M, Le T, Mallet E, Kottler ML. 2002. GNAS1 lesions in
13
14 492 pseudohypoparathyroidism Ia and Ic: genotype phenotype relationship and evidence
15
16 493 of the maternal transmission of the hormonal resistance. *J Clin Endocrinol Metab*
17
18 494 87:189-197.
- 19
20 495 Linglart A, Mahon MJ, Kerachian MA, Berlach DM, Hendy GN, Jüppner H, Bastepe M.
21
22 496 2006. Coding GNAS mutations leading to hormone resistance impair in vitro agonist-
23
24 497 and cholera toxin-induced cAMP formation mediated by human XL{alpha}s.
25
26 498 *Endocrinology* 147(5):2253-2262.
- 27
28 499 Mantovani G, Spada A. 2006. Mutations in the Gs alpha gene causing hormone resistance.
29
30 500 *Best Pract Res Clin Endocrinol Metab* 20; 501-513.
- 31
32 501 [Mantovani G, de Sanctis L, Barbieri AM, Elli FM, Bollati V, Vaira V, Labarile P, Bondioni](#)
33
34 502 [S, Peverelli S, Lania AG, Beck-Peccoz P, Spada A. 2010. Pseudohypoparathyroidism](#)
35
36 503 [and GNAS epigenetic defects: clinical evaluation of Albright hereditary](#)
37
38 504 [osteodystrophy and molecular analysis in 40 patients. J Clin Endocrinol Metab 95\(2\);](#)
39
40 505 [651-658.](#)
- 41
42 506 Masters SB, Sullivan KA, Miller RT, Beiderman B, Lopez NG, Ramachandran J, Bourne
43
44 507 HR. 1988. Carboxyl terminal domain of Gs alpha specifies coupling of receptors to
45
46 508 stimulation of adenylyl cyclase. *Science* 241:448-451.
- 47
48 509 Pantaloni C, Audigier Y. 1993. Functional domains of the Gs alpha subunit: role of the C-
49
50 510 terminus in the receptor-dependent and receptor-independent activation. *J Recept Res*

Deleted: a

- 1
2 511 13:591-608.
3
4 512 Rasenick MM, Watanabe M, Lazarevic MB, Hatta S, Hamm HE. 1994. Synthetic peptides as
5
6 513 probes for G protein function. Carboxyl-terminal G alpha s peptides mimic Gs and
7
8 514 evoke high affinity agonist binding to beta-adrenergic receptors. *J Biol Chem*
9
10 515 269:21519-21525.
11
12 516 Schwindinger WF, Miric A, Zimmerman D, Levine MA. 1994. A novel Gs alpha mutant in a
13
14 517 patient with Albright hereditary osteodystrophy uncouples cell surface receptors from
15
16 518 adenylyl cyclase. *J Biol Chem* 269:25387-25391.
17
18 519 Spiegel AM, Simonds WF, Jones TL, Goldsmith PK, Unson CG. 1990. Antibodies against
19
20 520 synthetic peptides as probes of G protein structure and function. *Soc Gen Physiol Ser*
21
22 521 45:185-195.
23
24 522 Sullivan KA, Miller RT, Masters SB, Beiderman B, Heideman W, Bourne HR. 1987.
25
26 523 Identification of receptor contact site involved in receptor-G protein coupling. *Nature*
27
28 524 330:758-760.
29
30 525 Sunahara RK, Tesmer JJG, Gilman AG, Sprang SR. 1997. Crystal structure of the adenylyl
31
32 526 cyclase activator Gs α . *Science* 278:1943-1947.
33
34 527 Weinstein LS. 1998. Albright hereditary Osteodystrophy, pseudohypoparathyroidism and Gs
35
36 528 deficiency. in: Spiegel AM ed. *G proteins, receptors, and disease*. New Jersey:
37
38 529 Humana Press; 23-56.
39
40 530 Weinstein LS, Chen M, Liu J. 2002. Gs(alpha) mutations and imprinting defects in human
41
42 531 disease. *Ann N Y Acad Sci* 968:173-197.
43
44 532 Zhang L, Bastepe M, Jüppner H, Ruan KH. 2006. Characterization of the molecular
45
46 533 mechanisms of the coupling between intracellular loops of prostacyclin receptor with
47
48 534 the C-terminal domain of the G α s protein in human coronary artery smooth muscle
49
50 535 cells. *Arch Biochem Biophys* 454:80-88.
51
52
53
54
55
56
57
58
59
60

536 **Figure legends:**537 **Figure 1) Stimulation of PHPIc associated missense mutants Gsα-388R and Gsα-392K,**538 **Panel a)** shows cAMP accumulation of both transfected missense mutants after receptor539 mediated stimulation of the endogenous expressed β₂-receptor due to Isoproterenol compared

540 to receptor-independent stimulation due to CTX. The mutation p.L388R results in a loss of

541 receptor-mediated stimulation, despite normal receptor-independent activation, compared to

542 the wild-type. The Gsα-392K mutant demonstrates a diminished activity after receptor-

543 mediated stimulation, although the receptor-independent stimulation is comparable to that of

544 the Gsα-wild-type. % max: maximal response after stimulation of the Gsα-wild type with

545 CTX. **Panel b)** Different concentrations of Isoproterenol (Iso) ranging from 10⁻⁸ to 10⁻⁴ M546 lead to a dose dependent stimulation of the β₂ receptor in the wild-type and the Gsα-392K547 mutant. The Gsα-388R mutant failed to induce intracellular cAMP synthesis. **Panel c)**

548 Similar results are shown after cotransfection with the PTHR: incubation with various

549 concentrations of human PTH ranging from 10⁻¹¹ to 10⁻⁷ M lead to a dose dependent response

550 for the wild-type, and the Gsα-392K mutant, whereas the Gsα-388R-mutant does not show

551 any response.

552

553 **Figure 2) PHPIc and PHPIa associated Gsα-mutants can be distinguished by in-vitro**554 **stimulation tests.** These experiments demonstrate that the cell model may be appropriate to

555 reflect differences in receptor-independent activation between PHPIc and PHPIa and between

556 the effects of missense and nonsense mutations: **Panel a)** In contrast to Gsα-388R, the Gsα-

557 388P mutant found in a patient with PHPIa leads to a clearly diminished CTX induced cAMP

558 synthesis that was significantly different from the corresponding cAMP levels in cells

559 expressing Gsα-388R (*P*<0.001). **Panel b)** After receptor-mediated stimulation the Gsα-392K

560 mutant revealed a residual activity that was absent in the nonsense mutant Gsα-392X

Deleted: both missense mutants
associated with PHPIc

Formatted: Font: Bold

Formatted: Font: Not Bold

Deleted: ,

Deleted: ,

Deleted: despite

Deleted: those

Deleted: Comparison of

Deleted: S

Deleted: stimulation results of

Deleted: 388R

Deleted: , compared to PHPIa
associated Gsα-388P mutant

Deleted: rest

Deleted: ,

1
2
3 561 | ($P < 0.001$), **Panel c** Comparison of Gs α -protein levels in non-transfected (n.t.) and
4
5 562 transfected Gnas^{E2-/E2-} cells by immunoblot analysis. Gs α -wild-type (WT), Gs α -388R
6
7 563 (388R), Gs α -388P (388P), Gs α -392K (392K), and Gs α -392X (392X). The protein levels of
8
9 564 the mutants were similar to those of the wild-type.

10
11 565
12
13 566 **Figure 3) Ribbon representation of Gs α in complex with GTP- γ s. Left:** The C-terminal
14
15 567 helix ($\alpha 5$) is colored in light blue, the helix $\alpha 4$ and the β -strand $\beta 6$ in green and the GTP- γ s
16
17 568 molecule is depicted as a ball and stick representation. C denotes the C-terminus. **Right:**
18
19 569 Close-up of the C-terminal region. The side chain of L388 is depicted and the hydrogen bond
20
21 570 between the amide group of L388 and the carbonyl group of Q384 is shown in red (dashed
22
23 571 line).

	PHPIa	PPHP	PHPIb	PHPIc
AHO features	yes	yes	rarely	yes
PTH resistance	yes	no	yes	yes
GNAS defects	mutations in exons 1-13	mutations in exons 1-13	epigenetic changes at the <i>GNAS</i> locus e.g. loss of methylation	not known, one mutation in exon 13 (Linglart et al., 2002)
<i>In-vitro</i> Gsa protein activity *	diminished	diminished	normal	normal
Transmission	maternal	paternal	maternal	maternal

Table 1) Subtypes of PHP and differences in phenotype, molecular genetic defects and *in-vitro* Gsa protein activity. The classification of PHP is based on the presence or absence of AHO features and the result of the Gs α protein activity carried out on isolated Gs α from erythrocyte membranes derived from patients. The result of the Gs α protein activity assay is the only certain difference between PHPIc and PHPIa, which is diminished in PHPIa and normal in PHPIc.

*normal range: 85-115%

Patient	A	B	C	D1	D2	E
Age at diagnosis, sex	12 years, male	5.5 years, female	11 month, female	13 years, male	13 years, female	4 years, female
Clinical features	rf, sst, bm, mr,o	rf, bm, o	rf, sst, bm	rf, bm	rf, bm, o	rf, bm, o
AHO Mother	sst, bm	bm	sst, bm	rf, sst, bm	rf, sst, bm	bm
PTH* (pg/ml; normal: 10-65)	416	133	138	643	544	286
Calcium (mmol/l; normal: 2.1-2.6)	0.84	1.1	normal	1.5	1.9	1.7
Phosphorous (mmol/l; normal: 1.09-2) age-dependent	3	2.7	2.3	3.3	2.3	3.1
TSH (mU/l; normal: 0.5-4)	9.3	6	4.7	5.9	7.4	4.5
ft3 (pg/ml; normal: 3.3-6.7)	normal	normal	normal	normal	normal	normal
ft4 (pg/ml; normal: 0.9-1.6)	normal	normal	normal	normal	normal	normal
Gsa activity in % of healthy controls (normal: 85-115)	108	102	108	100	105	71
Mutation**	c.1163T>G p.L388R	c.1174G>T p.E392X	c.1174G>A p.E392K	c.1174G>T p.E392X	c.1174G>T p.E392X	c.1163T>C p.L388P

Deleted: AHO

Deleted: (

Table 2) Phenotypical, laboratory results, *in-vitro* Gsa protein activity, and results of mutational analysis of our patients.

Deleted: ¶

Legend: rf: round face, sst: short stature, bm: brachymetacarpia, mr: mental retardation, o: obesity. Values in brackets define the normal range.

* all laboratory results at the time of initial diagnosis

**RefSeq: NM_000516.4

Nucleotide numbering reflects cDNA numbering system with +1 corresponding to the A of the ATG translation initiation codon in the reference sequence, according to the journal guidelines (www.hgvs.org/mutnomen).

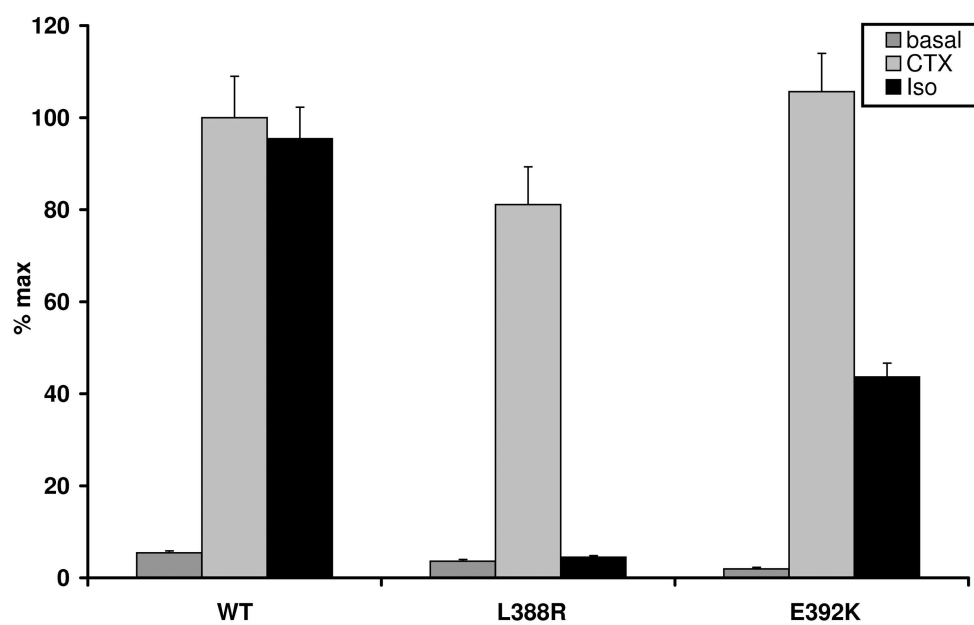
1
2
3
4
5
6
7
8
9
10
11
12
13
14
15
16
17
18
19
20
21
22
23
24
25
26
27
28
29
30
31
32
33
34
35
36
37
38
39
40
41
42
43
44
45
46
47
48
49
50
51
52
53
54
55
56
57
58
59
60

Drosophila melanogaster	DTENIKRVFNDCRDI I QRMHLRQYELL
Xenopus laevis	DTENIRRVFNDCRDI I QRMHLRQYELL
Mus musculus	DTENIRRVFNDCRDI I QRMHLRQYELL
Macaca mulatta	DTENIRRVFNDCRDI I QRMHLRQYELL
Homo sapiens	DTENIRRVFNDCRDI I QRMHLRQYELL

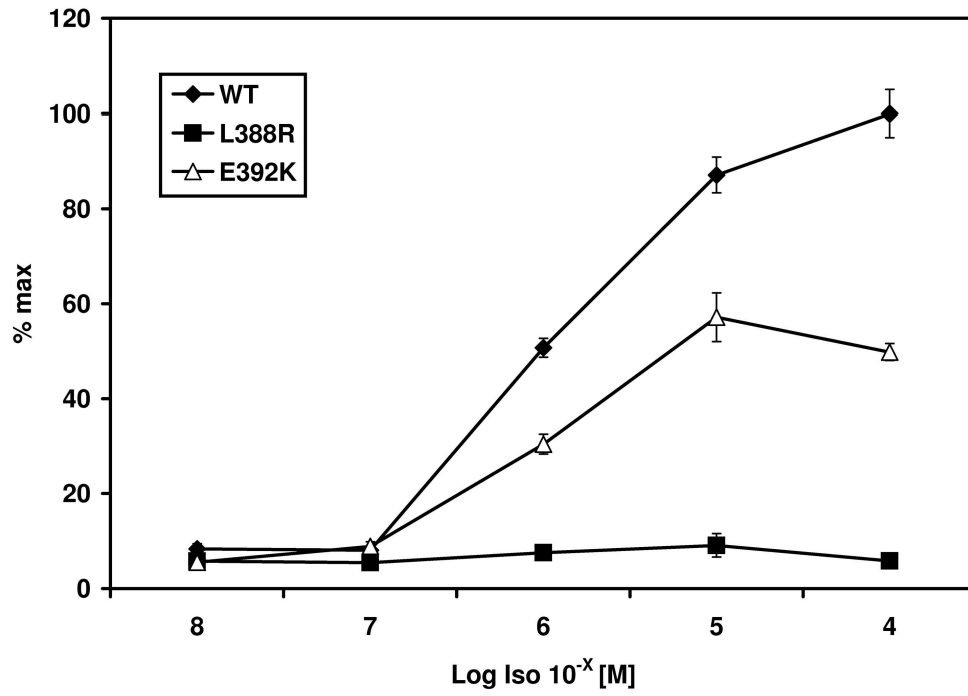
Table 3) Sequence alignment of the $\alpha 5$ helix of *Gsa* in different species. The C-terminus of

Gsa is highly conserved. Amino acid residues 388 and 392 are framed.

Deleted: Codon

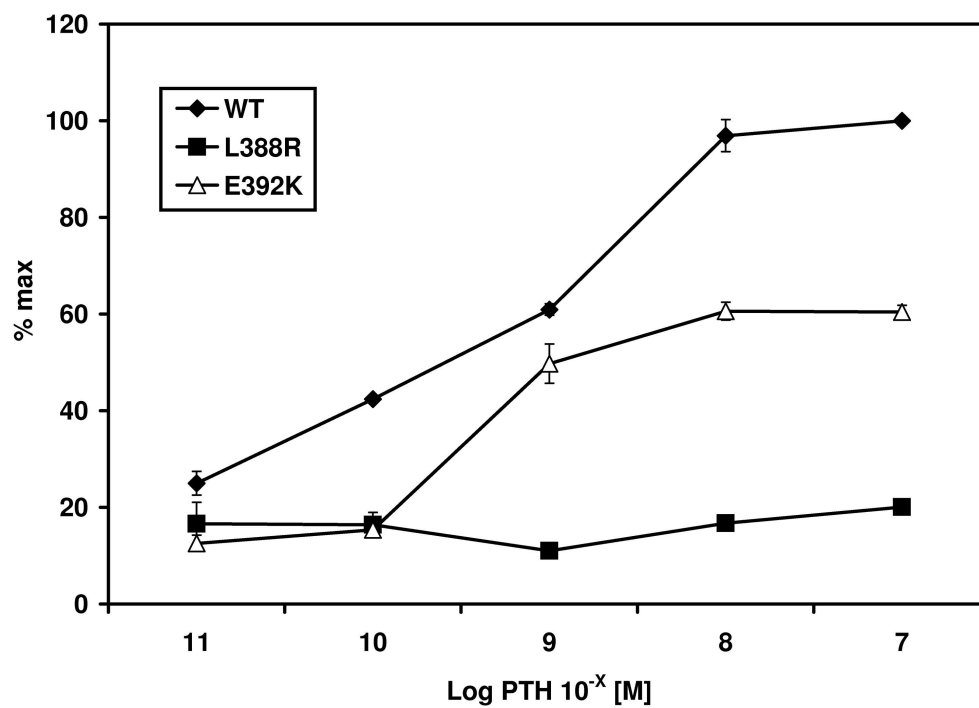


781x500mm (96 x 96 DPI)

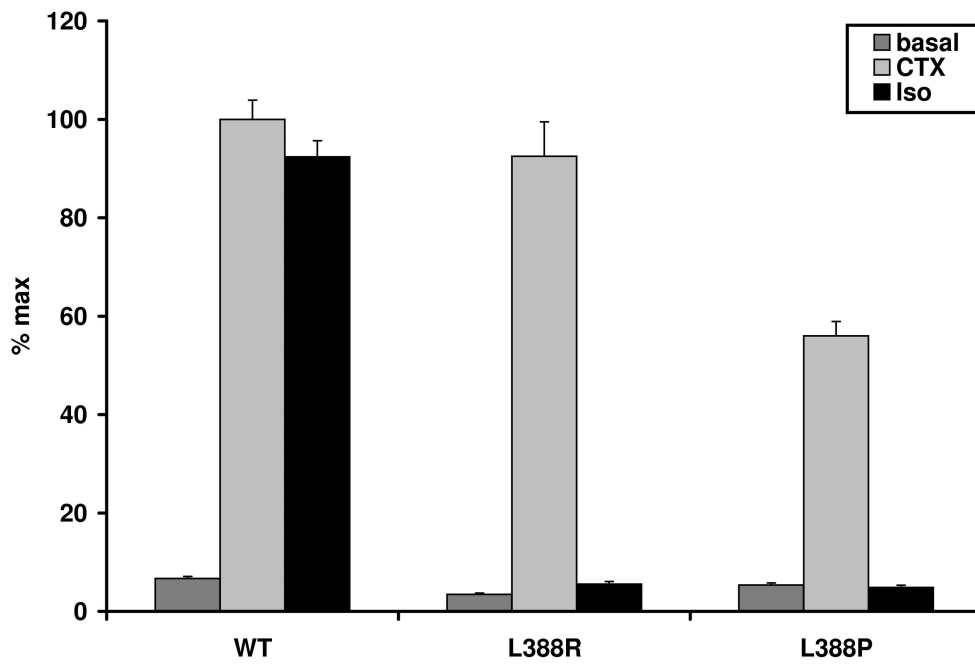


781x545mm (96 x 96 DPI)

Review

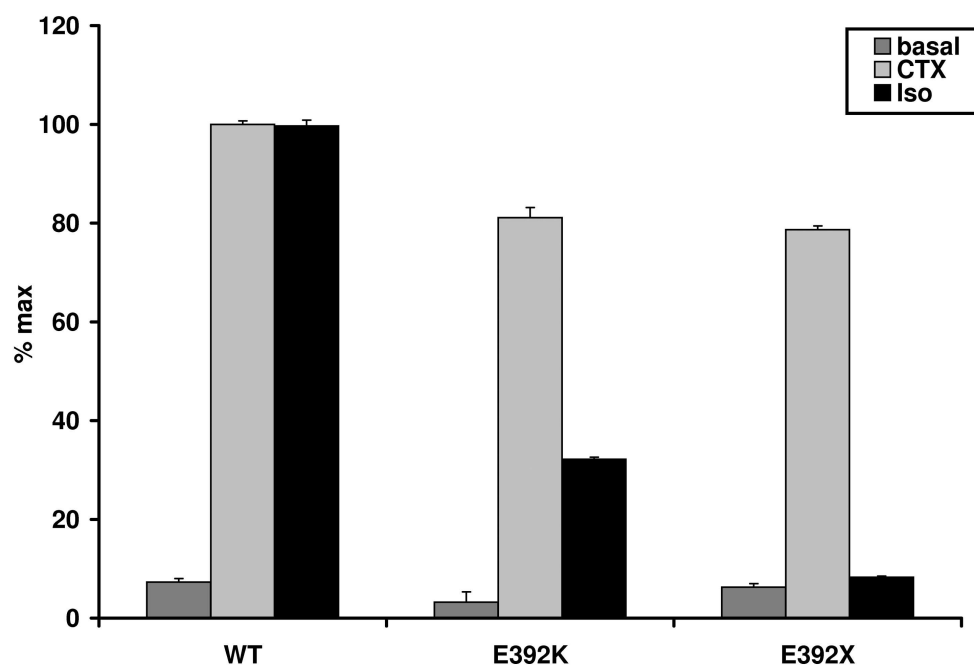


781x555mm (96 x 96 DPI)



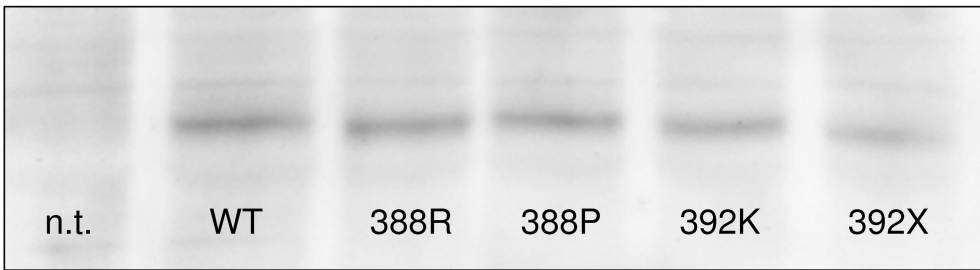
781x527mm (96 x 96 DPI)

Review



781x543mm (96 x 96 DPI)

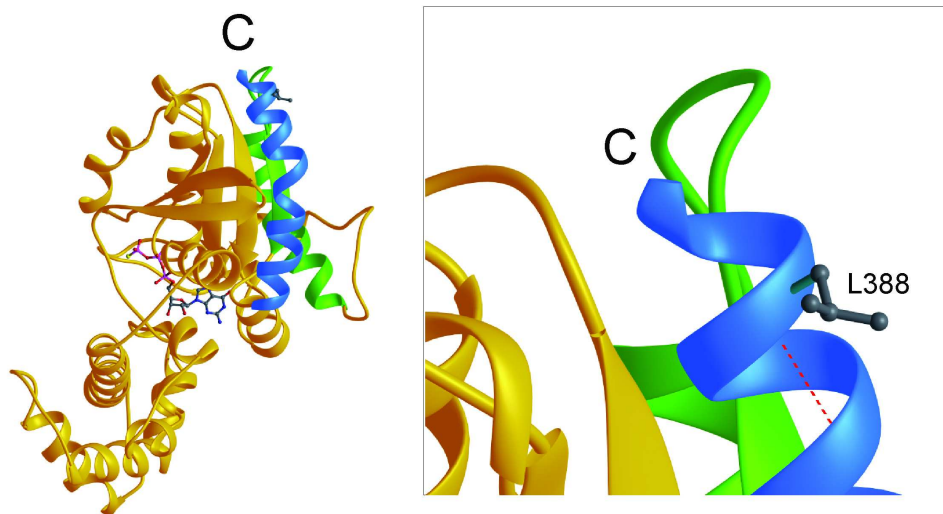
1
2
3
4
5
6
7
8
9
10
11
12
13
14
15
16
17
18
19
20
21
22
23
24
25
26
27
28
29
30
31
32
33
34
35
36
37
38
39
40
41
42
43
44
45
46
47
48
49
50
51
52
53
54
55
56
57
58
59
60



125x36mm (600 x 600 DPI)

For Peer Review

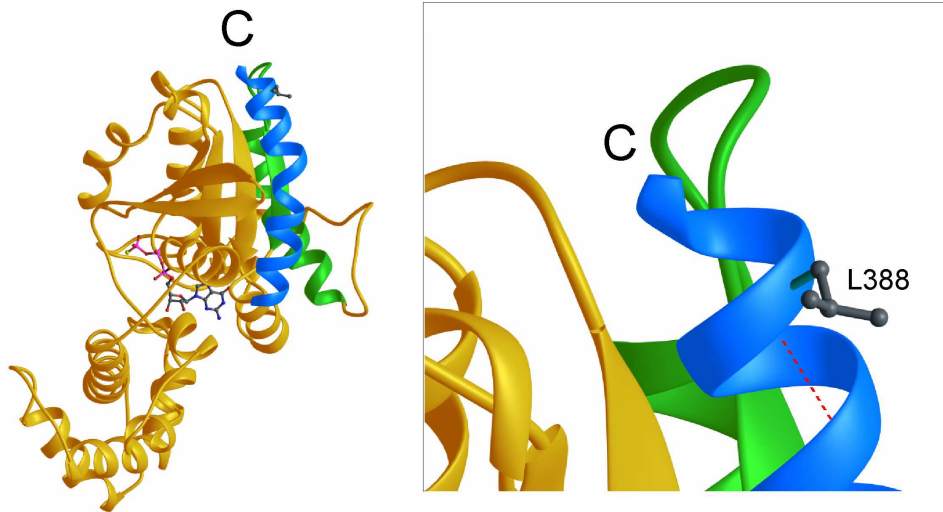
1
2
3
4
5
6
7
8
9
10
11
12
13
14
15
16
17
18
19
20
21
22
23
24
25
26
27
28
29
30
31
32
33
34
35
36
37
38
39
40
41
42
43
44
45
46
47
48
49
50
51
52
53
54
55
56
57
58
59
60



199x105mm (300 x 300 DPI)

Peer Review

1
2
3
4
5
6
7
8
9
10
11
12
13
14
15
16
17
18
19
20
21
22
23
24
25
26
27
28
29
30
31
32
33
34
35
36
37
38
39
40
41
42
43
44
45
46
47
48
49
50
51
52
53
54
55
56
57
58
59
60



199x105mm (300 x 300 DPI)

Peer Review